A comparative infrared spectroscopic study of glycoside hydrolases from extremophilic archaea revealed different molecular mechanisms of adaptation to high temperatures

10 AUTHORS, INCLUDING:

Alessio Ausili
Universidad Técnica Particular de Loja
41 PUBLICATIONS **290** CITATIONS

SEE PROFILE

Beatrice Cobucci-Ponzano
Italian National Research Council
51 PUBLICATIONS **552** CITATIONS

SEE PROFILE

Giuseppe Perugino
Italian National Research Council
39 PUBLICATIONS **732** CITATIONS

SEE PROFILE

Mosè Rossi
Italian National Research Council
305 PUBLICATIONS **5,482** CITATIONS

SEE PROFILE

A Comparative Infrared Spectroscopic Study of Glycoside Hydrolases From Extremophilic Archaea Revealed Different Molecular Mechanisms of Adaptation to High Temperatures

Alessio Ausili,[1] Beatrice Cobucci-Ponzano,[2] Barbara Di Lauro,[2] Rossana D'Avino,[2] Giuseppe Perugino,[2] Enrico Bertoli,[1] Andrea Scirè,[1] Mosè Rossi,[2,3] Fabio Tanfani,[1]* and Marco Moracci[2]

[1]*Institute of Biochemistry, Università Politecnica delle Marche, Via Ranieri, 60131 Ancona, Italy*
[2]*Institute of Protein Biochemistry, CNR, Via P. Castellino 111, 80131 Naples, Italy*
[3]*Department of Biological Chemistry, University of Naples "Federico II", Via Mezzocannone 16, 80134, Naples, Italy*

ABSTRACT The identification of the determinants of protein thermal stabilization is often pursued by comparing enzymes from hyperthermophiles with their mesophilic counterparts while direct structural comparisons among proteins and enzymes from hyperthermophiles are rather uncommon. Here, oligomeric β-glycosidases from the hyperthermophilic archaea *Sulfolobus solfataricus* (Ssβ-gly), *Thermosphaera aggregans* (Taβ-gly), and *Pyrococcus furiosus* (Pfβ-gly), have been compared. Studies of FTIR spectroscopy and kinetics of thermal inactivation showed that the three enzymes had similar secondary structure composition, but Ssβ-gly and Taβ-gly (temperatures of melting 98.1 and 98.4°C, respectively) were less stable than Pfβ-gly, which maintained its secondary structure even at 99.5°C. The thermal denaturation of Pfβ-gly, followed in the presence of SDS, suggested that this enzyme is stabilized by hydrophobic interactions. A detailed inspection of the 3D-structures of these enzymes supported the experimental results: Ssβ-gly and Taβ-gly are stabilized by a combination of ion-pairs networks and intrasubunit S-S bridges while the increased stability of Pfβ-gly resides in a more compact protein core. The different strategies of protein stabilization give experimental support to recent theories on thermophilic adaptation and suggest that different stabilization strategies could have been adopted among archaea. Proteins 2007;67:991–1001. © 2007 Wiley-Liss, Inc.

Key words: β-glycosidase; *Sulfolobus solfataricus*; *Thermosphaera aggregans*; *Pyrococcus furiosus*; protein structure; infrared

INTRODUCTION

The molecular mechanisms of protein stabilization are an interesting issue that have intrigued biochemists and biophysics for the past 20 years. The reason for these efforts is both for basic and applied research since the lack in the thermostability of proteins is one of the main factors limiting their industrial application. The identification of the determinants of thermal stabilization has been pursued by different methods; among the many, the comparison of enzymes from hyperthermophiles (thriving at temperatures above 80°C) with their mesophilic counterparts at structural, biochemical, and, more recently, genomic level[1–4] has led to the identification of a variety of stabilizing factors, including increased numbers of ion pairs, reduction in size of loops and cavities, reduced ratio of surface area to volume, additional proline residues in turns, increased hydrophobic interactions, and higher degree of oligomerization.[5,6] The comparison with the mesophiles applied to enzymes belonging to the glycoside hydrolase family 1 (GH1) (http://afmb.cnrs-mrs.fr/CAZY/), allowed to conclude that an increased number of ion-pairs could stabilize the enzymes from hyperthermophiles[7,8] while the β-glycosidase from the moderate thermophile *Thermus neoproteolyticus* HG102 revealed α-helix stabilization, restricted loop flexibility and increase in the number of ion-pairs and in Pro and Arg residues.[9]

Therefore, though the elements stabilizing the enzymes from hyperthermophiles have been studied in detail at molecular level, simple trends and mechanisms of stabilization common to enzymes from hyperthermo-

philes has not been unequivocally determined, suggesting that these organisms followed different routes to stabilize their proteins[10] leaving the problem of the stabilization of hyperstable enzymes still open. Furthermore, the number of studies dealing with detailed enzymatic comparisons among hyperthermophilic catalysts is remarkably low[11] and they are focused on evolutionary aspects.[4] Therefore, the question of how different hyperstable enzymes cope with temperatures near the boiling point of water still needs clarification.

The aim of our study was to compare at structural and functional level three archaeal enzymes belonging to family GH1 for which the three-dimensional (3D) structure is available, namely the β-glycosidases from the hyperthermophiles *Sulfolobus solfataricus* (Ssβ-gly), *Thermosphaera aggregans* (Taβ-gly), and *Pyrococcus furiosus* (Pfβ-gly). These proteins show high sequence similarity (sequence identity scores range between 52 and 60%), have the same tetrameric functional unit, a conserved catalytic dyad[12] and, since they belong to the same domain of living organisms, they represent an ideal model system to investigate the molecular basis of protein stability without evolutionary bias. The experiments of FTIR spectroscopy and the kinetics of thermal inactivation reported here revealed that Pfβ-gly is more stable than Ssβ-gly and Taβ-gly under all the conditions tested and that it is sensitive to incubations in the presence of SDS. These data, and the detailed inspection of the 3D-structures of these enzymes, allowed us to drive conclusions on their mechanisms of stabilization.

MATERIALS AND METHODS

Deuterium oxide (99.9% ^{2}H$_2$O) was purchased from Aldrich. All other reagents and solvents were commercial samples of the highest purity.

Preparation of Samples for Infrared Measurements

The enzymes were expressed in recombinant form and purified as reported previously.[12,13] In particular, the characteristics of Ssβ-gly and Pfβ-gly are similar to those of the native enzymes,[14,15] indicating that they can be used as reliable model systems for the study of protein stability. Typically, about 1.5 mg of Ssβ-gly or Taβ-gly, or Pfβ-gly, dissolved in the buffer used for their purification, were centrifuged in a "30K Centricon" micro concentrator (Amicon) at $3000 \times g$ and 4°C, and concentrated to a volume of approximately 40 μL. Then, 300 μL of 50 mM phosphate buffer (prepared in ^{2}H$_2$O), p^{2}H 6.5, were added and the sample concentrated again; the p^{2}H value corresponds to the pH-meter reading +0.4.[16] This procedure was repeated several times in order to completely replace the original buffer with the 50 mM phosphate buffer p^{2}H 6.5. In the last washing the protein sample was concentrated to a final volume of approximately 35 μL and used for the infrared measurements.

Pfβ-gly showed the tendency to aggregate at high concentration. Indeed, during the preparation of the Pfβ-gly sample, i.e. during the concentration and dilution procedure, the protein underwent partial precipitation. We analyzed both the precipitate and the protein that remained in solution. However, the addition of SDS prior to the concentration process subsequently avoided the precipitation of the protein. Hence, two samples were prepared in the presence of different amounts of SDS. In particular, the detergent was added once to 1.6 mL of protein solution to a final concentration of 0.2% sample (A) or 0.5% sample (B). The samples were concentrated to about 40 μL and then diluted by adding 300 μL of 50 mM phosphate buffer p^{2}H 6.5. The concentration and dilution procedure was then repeated several times as described above. Because of the formation of micelles, the majority of SDS remained in the micro concentrator during the concentration process. However, part of the detergent probably passed through the pores of the filter. Hence, the SDS concentration in the final concentrated protein samples was checked using a calibration curve obtained by monitoring the intensity of the SDS symmetric methylene stretching vibration band (2854 cm^{-1})[17] as a function of SDS concentration. The SDS resulted 1.2 and 5% in sample (A) and (B), respectively.

Infrared Spectra and Kinetics of Thermal Inactivation

The concentrated protein samples were placed in a thermostated Graseby Specac 20500 cell (Graseby-Specac, Orpington, Kent, UK) fitted with CaF$_2$ windows and a 25 μm Teflon spacer. FTIR spectra were recorded by means of a Perkin-Elmer 1760-x Fourier transform infrared spectrometer using a deuterated triglycine sulphate detector and a normal Beer-Norton apodization function. At least 24 h earlier and during data acquisition the spectrometer was continuously purged with dry air at a dew point of −70°C. Spectra of buffers and samples were acquired at 2 cm^{-1} resolution under the same scanning and temperature conditions. In the thermal denaturation experiments, the temperature was raised in 5°C steps from 20 to 95°C. The actual temperature in the cell was controlled by a thermocouple placed directly onto the CaF$_2$ window. Spectra were collected and processed using the "Spectrum" software from Perkin Elmer. The deconvoluted parameters for the amide I band were set with a gamma value of 2.5 and a smoothing length of 60. Second derivative spectra were calculated over a 9-data point range (9 cm^{-1}).

The temperature of melting (T_m) in thermal denaturation curves was calculated as described.[18]

Kinetics of thermal inactivation were performed as reported previously by using 0.1 mg/mL of each enzyme at the indicated temperatures.[19] Briefly, samples were incubated in sodium phosphate buffer 50 mM pH 6.5 in sealed tubes and taken at proper times, chilled in ice, and residual enzymatic activity was measured by following the β-galactosidase activity at 65°C in 50 mM sodium phosphate buffer at pH 6.5 with 4-nitrophenyl-β-D-galactopyranoside substrate at the final concentration of 5 mM. Activity of the sample before heat incubation was taken as 100%.
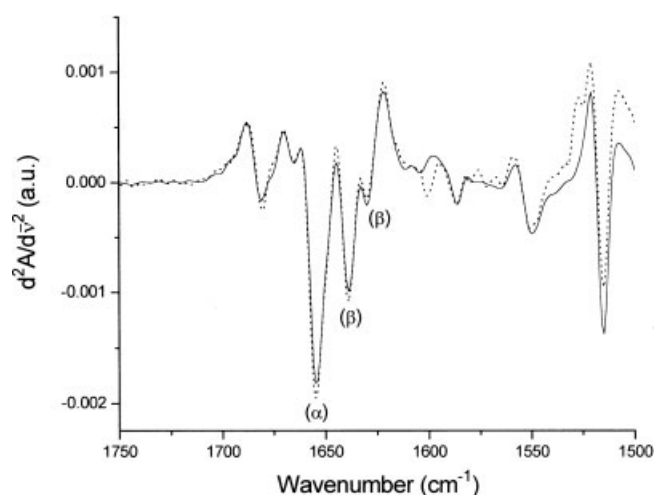
Fig. 1. Second derivative spectra of Pfβ-gly. The concentration of Pfβ-gly solution causes partial protein aggregation and precipitation. The precipitate and the protein that remained in solution were analyzed separately. Continuous and dotted lines refer to the insoluble and soluble part of Pfβ-gly, respectively. The spectra were obtained at 20°C. The symbols (α) and (β) stand for α-helix and β-sheet, respectively.

In Silico Analysis

Tetrameric assembly of Ssβ-gly and of Taβ-gly was generated using the DeepView/Swiss-PdbViewer Program[20] by applying the BIOMT transformations given in the pdb files to the crystallographic asymmetric unit (PDB code 1UQW and 1QVB, respectively).

Analysis of intersubunit H-bonds and salt bridges was performed on a Silicon Graphics O2 workstation by using the InsightII molecular modeling system from Accelrys (San Diego, USA) and with the program Protein Explorer.[21] Here, atoms of different charge (Arg NE, Arg NH, Lys NZ vs. Asp OD, Glu OE) are considered involved in a salt bridge when they are within 4.0 Å.

Measurements of surfaces, contact areas and volumes, and analysis of the cavities were performed by using the DeepView/Swiss-PdbViewer Program.[20] The solvent accessible surface and cavities area are measured as the contact surface between a solvent probe (1.4 Å diameter) and the molecule and computed using the Connolly surface algorithm. The buried hydrophobic surface area at the interface was estimated by subtracting the value computed for the tetramer from the sum of the values computed for dimers. Hydrogen bonds were calculated on a Silicon Graphics O2 workstation using the InsightII package considering, in the absence of hydrogen atoms, the distance between two heavy atoms ranging between 2.19 and 3.3 Å.

RESULTS AND DISCUSSION

Secondary Structure of Protein Samples

Figure 1 shows the second derivative spectra of the soluble and aggregated Pfβ-gly. The lack of differences in the amide I' (1700–1620 cm^{-1}) component bands indi-

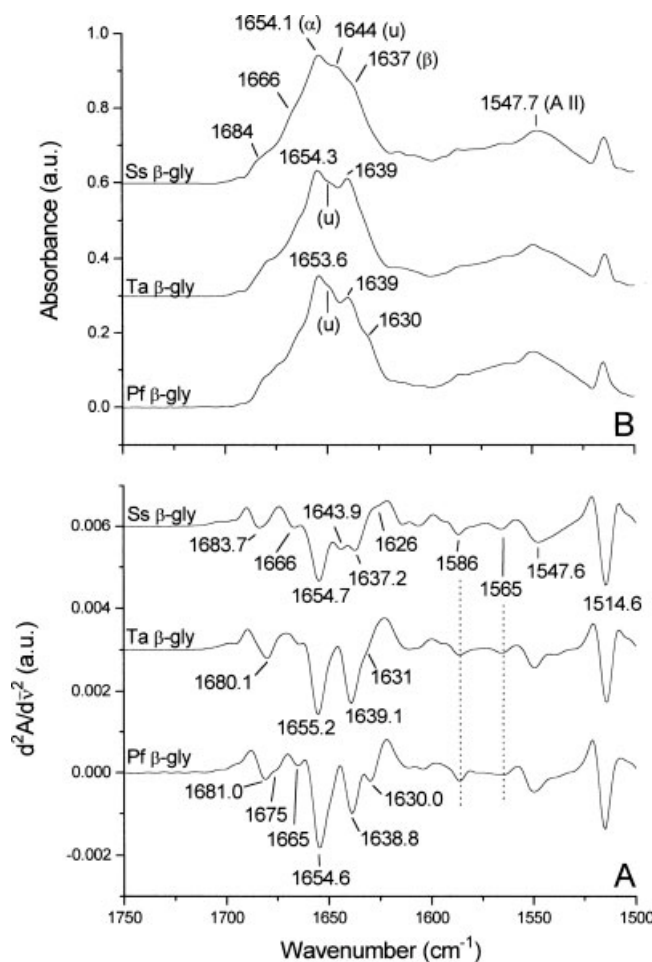Fig. 2. Second derivative (**A**) and deconvoluted (**B**) spectra of Ssβ-gly, Taβ-gly, and Pfβ-gly. The spectra were obtained at 20°C. The symbols (α), (β), (u), and (A II) stand for α-helix, β-sheet, unordered structures, and residual amide II band, respectively.

cates that the soluble and insoluble sample have the same secondary structure.

Figure 2 shows the second derivative (A) and deconvoluted (B) spectra of Ssβ-gly, Taβ-gly, and Pfβ-gly. All spectra display an α-helix band (close to 1655 cm^{-1}) and β-sheet bands (close to 1638 cm^{-1} and close to 1630 cm^{-1}).[22] These bands have different intensities and positions, suggesting that the β-glycosidases may have different secondary structure composition. The 1630 cm^{-1} band is well visible in Pfβ-gly, while in Taβ-gly and in Ssβ-gly it is present as a shoulder, which is very small in the case of the second derivative spectrum of Ssβ-gly. The band close to 1682 cm^{-1} is probably due to β-sheet, but it may contain information also on turns since both turns and coupled high frequency vibrations of β-segments can contribute in the 1670–1690 cm^{-1} spectral region.[23] The band close to 1665 cm^{-1} may be assigned to turns, while the absorption close to 1644 cm^{-1}, which is well visible only in the second derivative spectrum of Ssβ-gly, is due to unordered structures.[22] However, the presence of unordered structures in Taβ-gly and of Pfβ-gly is revealed by the
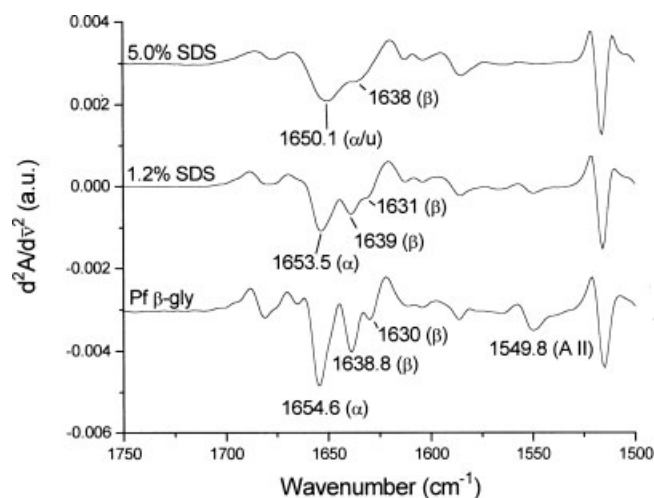
Fig. 3. Second derivative spectra of Pfβ-gly in the absence and presence of 1.2 or 5% SDS. The spectrum Pfβ-gly refers to the spectrum of the protein without SDS (control). The spectra were obtained at 20°C. The symbols (α), (β), (u), and (A II) stand for α-helix, β-sheet, unordered structures, and residual amide II band, respectively.

deconvoluted spectra, which show a shoulder at about 1644 cm^{-1}. The absorptions below 1620 cm^{-1} are due to amino acid side chain absorption[24] except for the band close to 1547 cm^{-1} that is due to residual amide II band i.e. to the absorption of the amide II band after $^1H/^2H$ exchange of the amide hydrogens of the polypeptide chain. In ^1H_2O medium the amide II band intensity is about 2/3 of the intensity of amide I band (data not shown), while in ^2H_2O medium its intensity decreases as a consequence of the exchange of amide hydrogens with deuterium.[25] The larger the decrease in intensity of the amide II band, the larger the $^1H/^2H$ exchange, that is the larger the accessibility of the solvent (^2H_2O) to the protein. Hence, the presence of the peak close to 1547 cm^{-1} indicates that part of amide hydrogens were not exchanged with deuterium during the preparation of the protein sample (see Materials and Methods). The band close to 1515 cm^{-1} is due to tyrosine residues, and the peaks close to 1565 and 1586 cm^{-1} are due to the ionized carboxyl groups of glutamic and aspartic acid, respectively.[24]

During the analysis of protein thermostability the denaturation of Pfβ-gly even at 99.5°C was never observed (see below). Hence, the protein was analyzed in the presence of SDS. Figure 3 compares the second derivative spectra of Pfβ-gly in the absence and in the presence of 1.2 or 5% SDS. The detergent affects the secondary structure of the protein since it induces changes in the intensity and position of the secondary structural element bands. These changes are SDS concentration-dependent. Indeed, in the presence of 5% SDS the band intensities are reduced remarkably and the 1630 cm^{-1} band is no longer visible. This is quite unusual since proteins from hyperthermophilic organisms often show a relevant stability and resistance towards common denaturants, including detergents. Indeed, in previous studies we showed that Ssβ-gly maintains its secondary
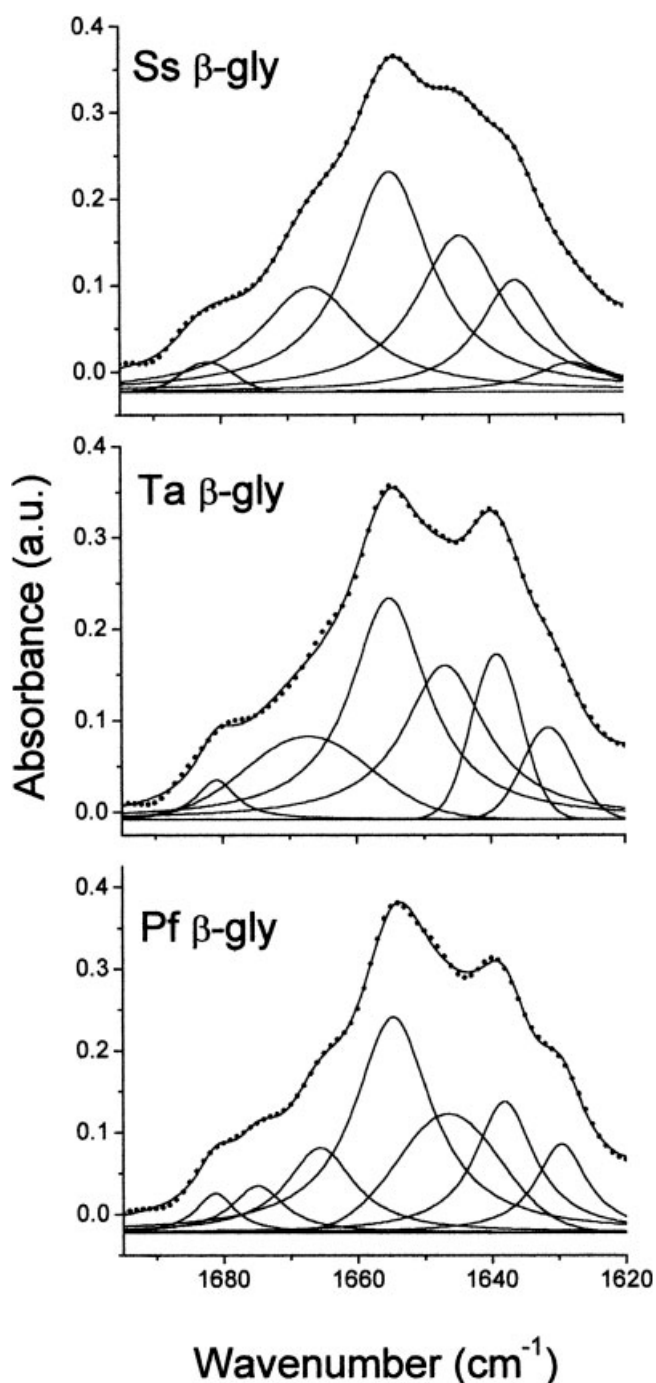
Fig. 4. Deconvoluted amide I′ band contour with the best fitted Gaussian/Lorentzian curves for Ssβ-gly, Taβ-gly, and Pfβ-gly. Chi square was 2.8 × 10^{-6}, 1.2 × 10^{-5}, and 9.5 × 10^{-6} for Ssβ-gly, Taβ-gly, and Pfβ-gly, respectively.

structure even in the presence of 5% SDS.[26] The residual amide II band intensity is also affected by the detergent. In the presence of 5% SDS it is not visible while in the presence of 1.2% SDS it is very small when compared to the control. Since the accessibility of the solvent (^2H_2O) to the protein increases when the protein undergoes denaturation or when its tertiary/quaternary structure

TABLE I. Calculated Positions and Fractional Areas (%) of the Amide I' Component Bands for Ssβ-gly, Taβ-gly, and Pfβ-gly

Ssβ-gly		Taβ-gly		Pfβ-gly	
Position	%	Position	%	Position	%
1627.7 (β)	3.9	1631.3 (β)	7.3	1629.6 (β)	9.7
1636.1 (β)	15.0	1639.1 (β)	12.5	1638.1 (β)	16.7
1644.3 (u)	25.2	1646.8 (u)	26.1	1646.4 (u)	18.6
1654.8 (α)	34.2	1655.1 (α)	35.1	1654.7 (α)	34.5
1666.5 (t)	19.2	1667.2 (t)	15.7	1665.6 (t)	12.0
1681.9 (β/t)	2.2	1680.2 (β/t)	3.3	1674.9 (β/t)	5.2
				1681.2 (β/t)	3.2

The symbols (α), (β), (u), (t), and (β/t) stand for α-helix, β-sheet, unordered structures, turns, and β-sheet and/or turns, respectively.

becomes less compact, the decrease in intensity of residual amide II band may be ascribed to a partial loss of secondary structures (Fig. 3) and/or to a relaxation of the Pfβ-gly tertiary/quaternary structure induced by SDS.

The composition of the secondary structure of the different protein samples was estimated by fitting the amide I' band with Gaussian/Lorentzian curves (Fig. 4). Table I reports the results of the curve-fitting calculations which confirm the different content of the low frequency β-sheets (band close to 1630 cm^{-1}) in the protein samples. On the other hand, Table I shows that the content in α-helix is the same in all proteins, and that the β-sheets belonging to the main β-sheet band (band close to 1638 cm^{-1}) are very similar.

Thermal Denaturation

The changes in the infrared spectrum induced by the temperature increase may reflect different phenomena. Typically, as shown in Figure 5, the temperature-dependent decrease in intensity of the α-helix and β-sheet bands are due to unfolding (denaturation) of these structural elements whilst the appearance of two new bands close to 1618 and 1684 cm^{-1} are characteristic of protein aggregation (intermolecular interaction) brought about by protein denaturation.[13,27] On the other hand, the temperature-dependent decrease in intensity of the residual amide II band (close to 1550 cm^{-1}) is due to further ^{1}H/^{2}H exchange caused by the temperature-dependent protein dynamics and/or protein denaturation.[13] Figure 5 shows that the increase in temperature leads to denaturation and aggregation of Ssβ-gly and Taβ-gly, but not of Pfβ-gly. Indeed, both in Ssβ-gly and in Taβ-gly it is possible to observe a large decrease in intensity of the amide I' band in the 90–99.5°C temperature range and a concomitant increase in intensity of the bands close to 1618 and 1684 cm^{-1} reflecting denaturation and aggregation of the proteins. Moreover, in correspondence of protein denaturation (90–99.5°C), the decrease in intensity of the residual amide II band becomes greater because of protein unfolding. At temperatures between 20 and 90°C, the decrease in intensity of the residual
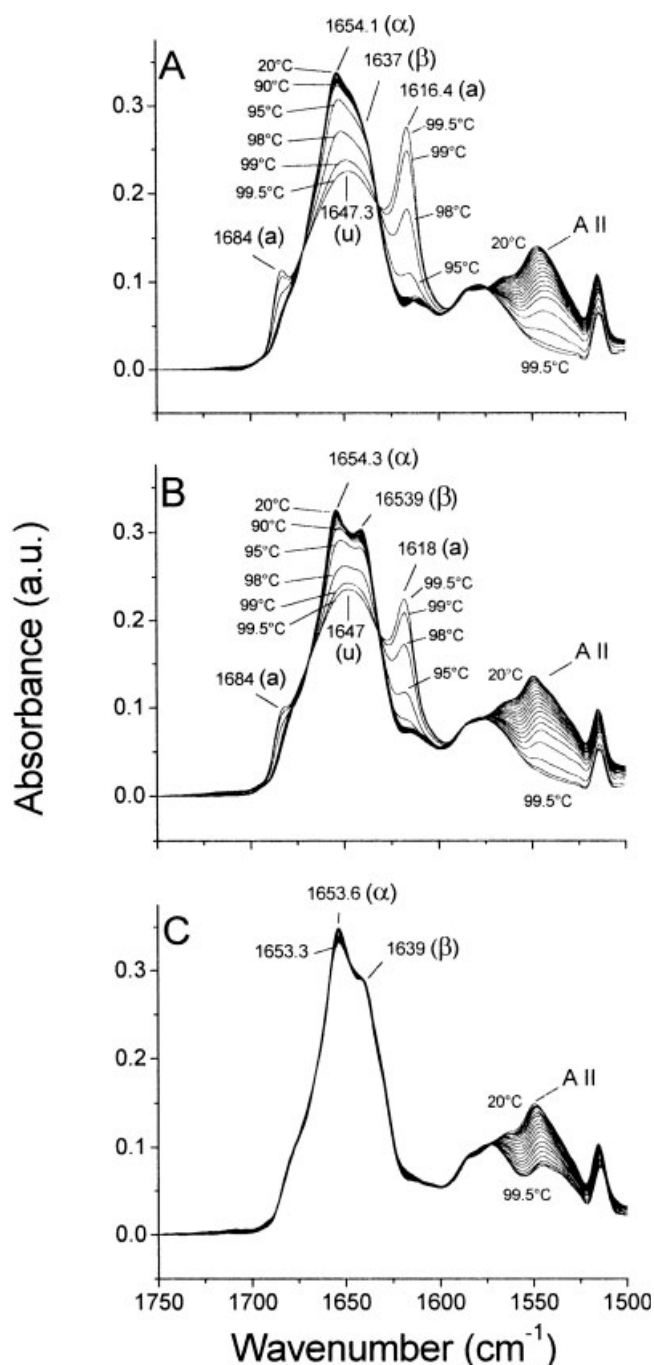
Fig. 5. Temperature-dependent changes in the deconvoluted infrared spectra of Ssβ-gly (**A**), Taβ-gly (**B**), and Pfβ-gly (**C**). In each panel, 16 spectra in the 20–95°C interval are shown, starting from 20 to 95°C with 5°C increments. Spectra recorded at 98, 99, and 99.5°C are also shown. The symbols (α), (β), (a), and (A II) stand for α-helix, β-sheet, aggregation, and residual amide II band, respectively.

amide II band is almost constant, most likely due to changes in molecular dynamics induced by the increase in temperature.

In the case of Pfβ-gly, the increase in temperature does not lead to a large decrease in intensity of the amide I' component bands, indicating that the protein is

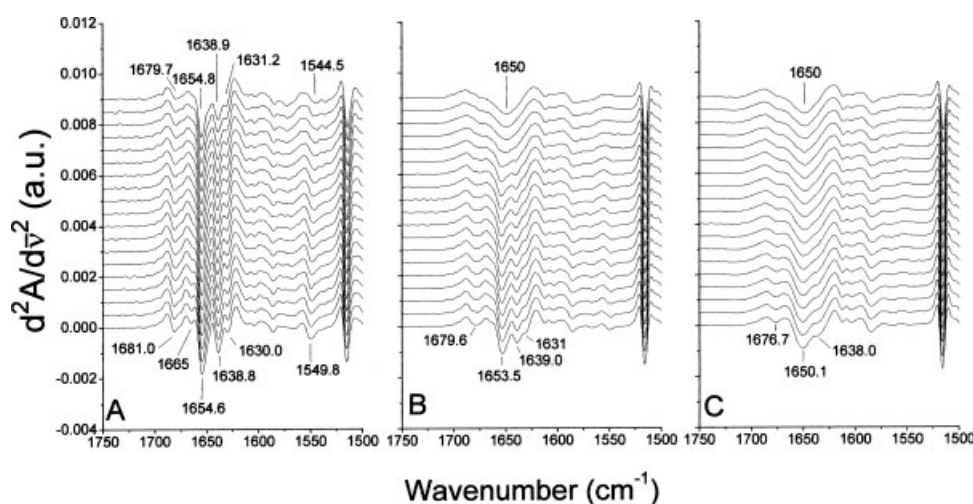Fig. 6.   Temperature-dependent changes in the second derivative infrared spectra of Pfβ-gly in the absence (**A**) and in the presence of 1.2% SDS (**B**) or 5% SDS (**C**). In each panel, 16 spectra in the 20–95°C interval are shown, starting from 20°C (bottom) to 95°C (top) with 5°C increments. Spectra recorded at 98, 99, and 99.5°C are also shown.

stable even at 99.5°C. Conversely, the increase in temperature causes a constant decrease in intensity of the residual amide II band due to increased molecular dynamics. It is worth nothing that at 99.5°C the residual amide II band is still visible (compare the Ssβ-gly, Taβ-gly, and Pfβ-gly spectra). This finding may be due to the fact that the protein retains its secondary structure and that it is particularly compact, and/or that some segments may be particularly buried. These data are in agreement with the experiments of differential scanning calorimetry showing that the temperature of melting (T_m) of this enzyme was 108°C.[28] Thermal denaturation curves for Ssβ-gly and Taβ-gly were obtained by plotting the changes of the amide I′ bandwidth as a function of the temperature[29,30] (data not shown). The temperature of melting for Ssβ-gly and Taβ-gly resulted 98.1 and 98.4°C, respectively and was calculated as described.[18]

This trend of thermal stability is confirmed also by kinetics of thermal inactivation. The activity of protein samples of Ssβ-gly, incubated for increasing times at 90 and 95°C, showed half-lives of 38 and 3 min, respectively; under the same conditions Taβ-gly showed a stability 2.4-fold higher at both 90 and 95°C (92 and 7 min, respectively). In striking contrast, Pfβ-gly resulted much more stable and no inactivation was observed at 90°C while at 95°C this enzyme showed an half-life of 225 min, which is 75- and 32-fold higher than those of Ssβ-gly and Taβ-gly, respectively, at the same temperature. It is worth noting that the thermal inactivation is coupled to protein aggregation for all the proteins tested.

The thermal denaturation of Pfβ-gly could be followed only in the presence of SDS. Figure 6 shows the second derivative spectra of Pfβ-gly in the absence and presence of 1.2 or 5% SDS, and at different temperatures. In the absence of detergent the enzyme retains its secondary structure at all temperatures while the spectra show

only a decrease in intensity of the residual amide II band confirming the data reported in Figure 5(C). In the presence of 1.2% SDS the amide I′ component bands are well visible at 20°C although they display different intensities with respect to the control (see also Fig. 3), indicating that the detergent affects the secondary structure of the protein. With the increase in temperature the amide I′ component bands decrease significantly in intensity starting from 90°C while at 95°C the bands are no longer visible. At 99.5°C, the spectrum is characterized by a broad band, centered at 1650 cm^{-1}, which appears after the loss of the secondary structural elements of the protein. The presence of this band is unusual for a completely denatured protein since its position is characteristic for α-helices. However, this band was previously observed in the presence of high SDS concentration and at high temperatures in β-galactosidase[31] and also in Ssβ-gly.[26] It was assigned to α-helices with the possible contribution of unordered structures. In the case of Ssβ-gly, the assignment of the 1650 cm^{-1} band to α-helices was supported also by the CD measurements that showed a high α-helix content in the presence of 5.0% SDS at 95°C.[26] In the presence of 5% SDS the spectrum of the protein at 20°C does not display the secondary structural elements as in the case of the control spectrum, indicating that a high SDS concentration induces a partial loss of the secondary structure. With the increase in temperature, the spectrum contour changes reflecting denaturation. However, the changes are less visible as compared to the control or to the spectrum in the presence of 1.2% SDS. Indeed, the disappearance of the 1638 cm^{-1} band seems to occur at about 55–60°C. In the case of the 1650.1 cm^{-1} band the identification of the temperature of its disappearance is less certain since at 99.5°C a 1650 cm^{-1} band, most likely due to unordered structures and α-helix induced by the SDS binding, is also present.

Figure 6 also shows that at high temperatures and in the presence of SDS the two bands characteristic of intermolecular interactions (aggregation) brought about by protein denaturation [see Fig. 5(A,B)] are lacking. This phenomenon may be explained by the fact that the binding of SDS to protein segments endows the polypeptide with additional negative charges that keep the polypeptide molecules apart, thereby avoiding intermolecular aggregation.[26]

Analysis of the 3D-Structures

In an effort to find a rational to explain the different stabilities of the glycosidases studied here, we analyzed the 3D-structures available for these enzymes. The 3D-structure of Ssβ-gly has recently been resolved at 1.95 Å[32] and it is deposited in the Brookheaven Protein Data Bank as 1UWQ while the structure of Taβ-gly (1QVB) is available at 2.4 Å.[8] Finally, the structure of Pfβ-gly (CelB) was a 3.3 Å structural model[33] obtained by molecular replacement from the structure of Ssβ-gly previously obtained at 2.6 Å.[7] It must be pointed out that the mid-level resolution at 3.3 Å of the 3D-structure of the *P. furiosus* enzyme does not allow to drive conclusive remarks on the structural details of this enzyme, therefore, the inspection of the structure of this enzyme reported below was performed to find a structural basis to the experimental data.

Preliminary analyses strongly indicated that the three enzymes had similar functional features summarized in Table II; in particular, the differences in terms of the surface and the volume of the tetrameric functional units were below 5%. This observation is also confirmed by the superimposition of the tetramers that for the couples 1UWQ-1QVB and 1UWQ-CelB produced r.m.s. of 1.64 and 0.69 Å, respectively, suggesting that the global folding of the three enzymes was almost identical. The only striking difference clearly observable is the presence of loops in the β-glycosidases from *S. solfataricus* and *T. aggregans*, which are missing in Pfβ-gly. This also explains the different length of the two former proteins in comparison with the β-glycosidase from *P. furiosus* (Table II).

The inspection of most of the structural elements that are reported as possible protein stabilizing features revealed interesting differences among the three β-glycosidases (Table III). In fact, Taβ-gly is the only enzyme showing a S-S bridge involving the residues Cys343 and Cys353 in each subunit while Ssβ-gly showed the highest number of salt bridges per functional unit and between surfaces. These findings are not surprising. The presence of large networks of ion-pairs has been recognized as one of the main determinants of the stability of enzymes from hyperthermophiles[34] and in Ssβ-gly this was experimentally proved.[19] Furthermore, the presence of an intrasubunit cystein bridge has been proposed as a possible reason for the increased stability of Taβ-gly over Ssβ-gly.[8] In addition, these enzymes showed larger contact surfaces between the two different monomer–mono-
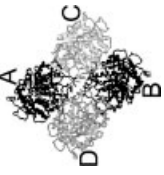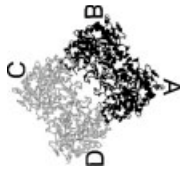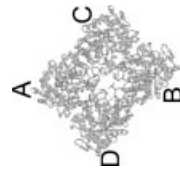
TABLE II. Comparison of Structural Features Among Hyperthermophilic GH1 β-Glycosidases

Enzyme	Number of residues	Functional unit	Number of α-helices[a]	Number of strands[a]	Number of turns[a]	Total surface (Å²)[a]	Total volume (Å³)[a]	Monomer average surface (Å²)[a]	Monomer average volume (Å³)[a]
Ssβ-gly	489	Tetramer	96	118	190	56,981	272,129	15,705 ± 117	66,955 ± 177
Taβ-gly	481	Tetramer	100	116	188	58,422	266,663	15,637 ± 60	65,845 ± 39
Pfβ-gly	472	Tetramer	108	120	172	59,920	259,922	15,801 ± 78	64,339 ± 93

[a]Data were calculated by using the program Swiss PDB Viewer.[20]

TABLE III. Comparison of the Putative Stabilizing Interactions in the Structures of Hyperthermophilic GH1 β-Glycosidases

Enzyme	Symmetries in the functional unit[a]	Number of prolines	Number of S-S	Number of intersubunit H-bonds	Number of salt-bridges in the monomer[b]	Number salt-bridges in the functional unit[b]	Number of intersubunit salt-bridges[b]	Surface between non-crystallographic monomers (Å²)[c]	Number of internal cavities per functional unit[c,d]	Average size of the internal cavities (Å²)[c,d]
Ssβ-gly		26	0	14 at interface AC[e] 14 at interface AD[f] 2 at interface AB	33	138	14	1,390 at interface AC[e] 1,118 at interface AD[f]	13	178 ± 83
Taβ-gly		30	1	13 at interface AB[g] 5 at interface AD[h] none at interface AC	25	114	12	871 at interface AD 1,194 at interface CD	14	186 ± 68
Pfβ-gly		24	0	6 at interface AC[e] 7 at interface AD[f] none at interface AB	21	92	8	945 at interface AC[e] 658 at interface AD[f]	5	153 ± 34

[a]The crystallographic dimers are shown in black; figures were prepared with the program RasMol.[39]
[b]Data were calculated by using the program Protein Explorer.[21]
[c]Data were calculated by using the program Swiss PDB Viewer.[20]
[d]Cavities ≥ 100 Å² were considered.
[e]The same at interface BD.
[f]The same at interface BC.
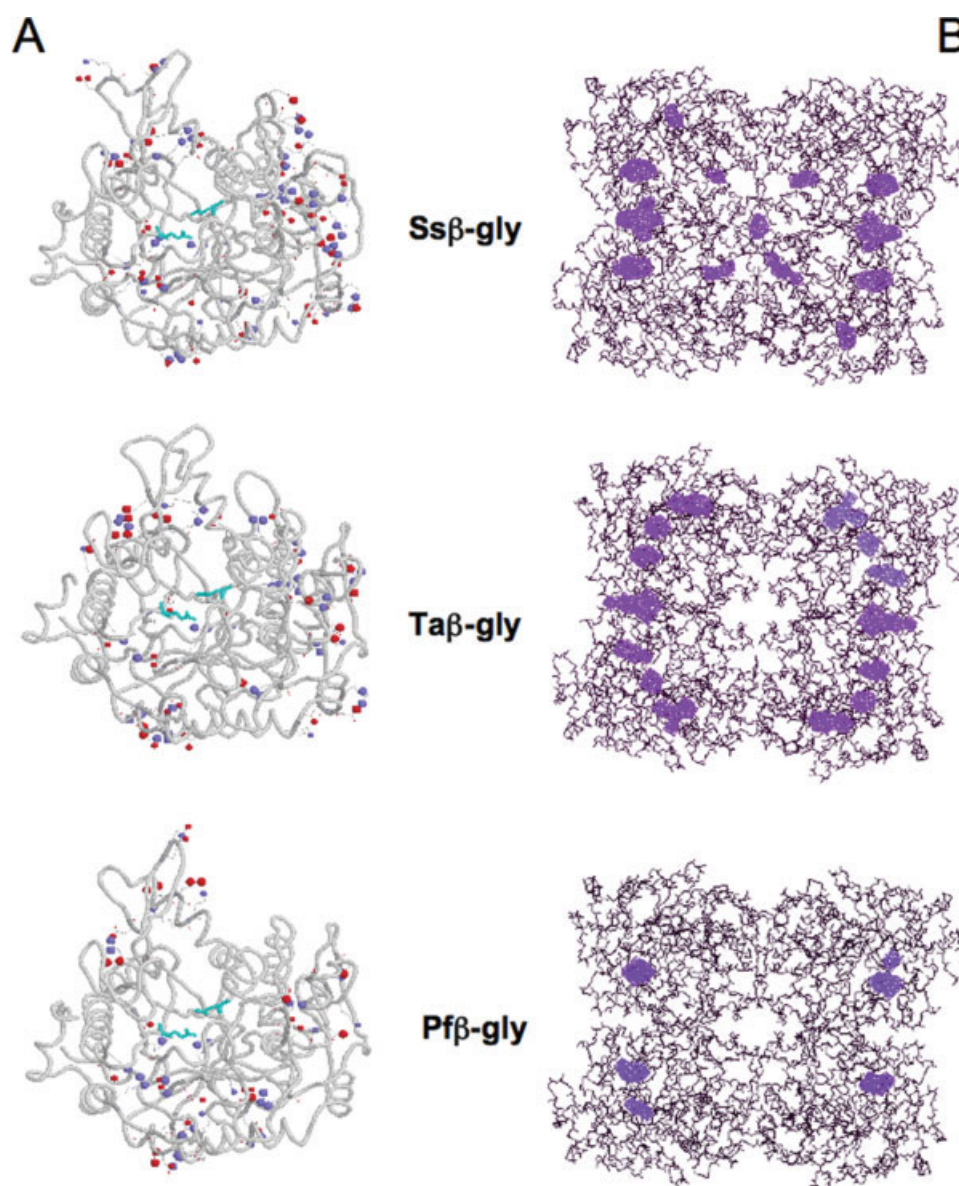[g]The same at interface CD.
[h]The same at interface BC.

Fig. 7.   Structural comparison of archaeal β-glycosidases. **A**: The monomers of the three enzymes show cationic and anionic atoms in blue and red respectively. The catalytic diads are shown as sticks in cyan. Images were prepared with the program Protein Explorer.[21] **B**: The tetramers of the three enzymes show internal cavities larger than 100 Å^2. Images were prepared with the program Swiss PDB Viewer.[20]

mer interfaces and an increased number of hydrogen bonds if compared to the enzyme from *P. furiosus* (Table III). This confirms the observation that oligomerization can play a relevant role in protein stabilization.[13]

The analysis of the 3D-structure suggested that the higher stability of Pfβ-gly could be obtained by means of different molecular mechanisms, since this enzyme showed few intersubunit contacts in terms of H-bonds, ion-pairs, and surfaces between adjacent monomers (Table III). In addition, in Pfβ-gly the ion-pairs per subunit are reduced by 1.5- and 1.2-fold if compared to Ssβ-gly and Taβ-gly, respectively (see Fig. 7). However, we found a striking reduction in the number of internal cavities of

Pfβ-gly *vs* Ssβ-gly and Taβ-gly, though the average size of these cavities is only slightly different (Table III and Fig. 7). This observation would indicate that the hydrophobic core of Pfβ-gly is much more compact than that of the enzymes from *S. solfataricus* and *T. aggregans*. Unfortunately, the limited resolution of the Pfβ-gly 3D-structure did not allowed us to conclude that the higher stability of this enzyme unequivocally result from the reduced number of ion-pairs and internal cavities. In fact, we cannot exclude that the 3.3 Å resolution affected these features. However, it is worth noting that these observations go in agreement with the thermal denaturation IR data (Fig. 5), which suggested a particular

compact structure and deeply buried protein segments. Protein interiors are tightly packed and buried apolar side chains influence protein stability through the hydrophobic effect that favors the shielding of apolar residues from water; in addition, packing interactions are thought to give rise to van der Waals stabilization of the native state.[35] Protein engineering studies demonstrated that cavities-creating mutations are generally destabilizing[36,37]; this suggests that the reduction in both the number and size of the internal cavities in the hydrophobic core of Pfβ-gly greatly contributed to its stability.

The experimental observation that the thermal stability of Pfβ-gly was reduced in the presence of SDS (see above) further supports the hypothesis that the stability of this enzyme is mainly driven by the compactness of the hydrophobic core and strikingly contrasts with the increased stability of Ssβ-gly in the presence of SDS.[26] Presumably, the alkyl chains of SDS have a marked destabilizing effect on the hydrophobic core of the enzyme from *P. furiosus* increasing its rate of thermal denaturation. It is worth noting that SDS had a similar effect on a protein disulfide oxidoreductase from the same source[38] and it has been reported that the extreme stability of a rubredoxin from the same organism is provided by the increased compactness of its structure.[4] Remarkably, high-throughput analyses and computational studies from these authors demonstrated that this is a general method of stabilization of proteins from *P. furiosus*, and they propose that the increment in packaging of the protein core could be the result of an evolutionary strategy of stabilization occurring in archaea. This mechanisms of stabilization, named "structure-based" counterpoises to a "sequence-based" mechanisms encountered in hyperthermophilic bacteria, in which a small number of point mutations (especially leading to an increase number of ion-pairs) are, apparently, responsible of the stability of the proteins from this source.[4] The different strategy of stabilization would result from the evolutionary history of the two groups of organisms: hyperthermophilic archaea originated in extreme environments while hyperthermophilic bacteria recolonized hot environments. Therefore, archaea enzymes were de novo designed in an hot abitat and were subjected to a bias toward certain structures and sequences that have to fold and be stable at high temperatures. Instead, the adaptation of hyperthermophilic enzymes from bacteria would be acquired by enhancing the thermostability of existing proteins of mesophilic origin. In these respects, our data, though referring to a limited number of proteins, confirmed the observation of Berezovsky and Shakhnovich experimentally demonstrating these mechanisms of stabilization. Nevertheless, our results indicate that this picture might be even more complicated since different stabilization methods could have been adopted among archaea. In fact, Ssβ-gly and Taβ-gly showed a "sequence-based" stabilization strategy while Pfβ-gly apparently followed a "structure-based" mechanism; further genomic and proteomic studies might help in shedding light on this intriguing issue.

REFERENCES

1. Vetriani C, Maeder DL, Tolliday N, Yip KS, Stillman TJ, Britton KL, Rice DW, Klump HH, Robb FT. Protein thermostability above 100 degrees °C: a key role for ionic interactions. Proc Natl Acad Sci USA 1998;95:12300–12305.
2. Bell GS, Russell RJ, Connaris H, Hough DW, Danson MJ, Taylor GL. Stepwise adaptations of citrate synthase to survival at life's extremes. From psychrophile to hyperthermophile. Eur J Biochem 2002;269:6250–6260.
3. Suhre K, Claverie JM. Genomic correlates of hyperthermostability, an update. J Biol Chem 2003;278:17198–17202.
4. Berezovsky IN, Shakhnovich EI. Physics and evolution of thermophilic adaptation. Proc Natl Acad Sci USA 2005;102:12742–12747.
5. Sterner R, Liebl W. Thermophilic adaptation of proteins. Crit Rev Biochem Mol Biol 2001;36:39–106.
6. Vieille C, Zeikus GJ. Hyperthermophilic enzymes: sources, uses, and molecular mechanisms of thermostability. Microbiol Mol Biol Rev 2001;65:1–43.
7. Aguilar CF, Sanderson I, Moracci M, Ciaramella M, Nucci R, Rossi M, Pearl LH. Crystal structure of the beta-glycosidase from the hyperthermophilic archeon Sulfolobus solfataricus: resilience as a key factor in thermostability. J Mol Biol 1997;271:789–802.
8. Chi YI, Martinez-Cruz LA, Jancarik J, Swanson RV, Robertson DE, Kim SH. Crystal structure of the beta-glycosidase from the hyperthermophile Thermosphaera aggregans: insights into its activity and thermostability. FEBS Lett 1999;445:375–383.
9. Wang X, He X, Yang S, An X, Chang W, Liang D. Structural basis for thermostability of beta-glycosidase from the thermophilic eubacterium Thermus nonproteolyticus HG102. J Bacteriol 2003; 185:4248–4255.
10. Petsko GA. Structural basis of thermostability in hyperthermophilic proteins, or "there's more than one way to skin a cat". Methods Enzymol 2001;334:469–478.
11. Pouwels J, Moracci M, Cobucci-Ponzano B, Perugino G, van der Oost J, Kaper T, Lebbink JH, de Vos WM, Ciaramella M, Rossi M. Activity and stability of hyperthermophilic enzymes: a comparative study on two archaeal beta-glycosidases. Extremophiles 2000;4:157–164.
12. Perugino G, Trincone A, Giordano A, van der Oost J, Kaper T, Rossi M, Moracci M. Activity of hyperthermophilic glycosynthases is significantly enhanced at acidic pH. Biochemistry 2003;42:8484–8493.
13. Ausili A, Di Lauro B, Cobucci-Ponzano B, Bertoli E, Scirè A, Rossi M, Tanfani F, Moracci M. Two-dimensional IR correlation spectroscopy of mutants of the beta-glycosidase from the hyperthermophilic archaeon Sulfolobus solfataricus identifies the mechanism of quaternary structure stabilization and unravels the sequence of thermal unfolding events. Biochem J 2004;384:69–78.
14. Moracci M, Nucci R, Febbraio F, Vaccaro C, Vespa N, La Cara F, Rossi M. Expression and extensive characterization of a beta-glycosidase from the extreme thermoacidophilic archaeon Sulfolobus solfataricus in Escherichia coli: authenticity of the recombinant enzyme. Enzyme Microb Technol 1995;17:992–997.
15. Voorhorst WG, Eggen RI, Luesink EJ, de Vos WM. Characterization of the celB gene coding for beta-glucosidase from the hyperthermophilic archaeon Pyrococcus furiosus and its expression and site-directed mutation in Escherichia coli. J Bacteriol 1995;177:7105–7111.
16. Salomaa P, Schaleger LL, Long FA. Solvent deuterium isotope effects on acid-base equilibria. J Am Chem Soc 1964;86:1–7.
17. Bellamy LJ, editor. The Infrared Spectra of Complex Molecules. London: Chapman and Hall; 1975.

18. Meersman F, Laszlo S, Heremans K. Comparative Fourier transform infrared spectroscopy study of cold-, pressure-, and heat-induced unfolding and aggregation of myoglobin. Biophys J 2002; 82:2635–2644.
19. Cobucci-Ponzano B, Moracci M, Di Lauro B, Ciaramella M, D'Avino R, Rossi M. Ionic network at the C-terminus of the beta-glycosidase from the hyperthermophilic archaeon Sulfolobus solfataricus: functional role in the quaternary structure thermal stabilization. Proteins 2002;48:98–106.
20. Guex N, Peitsch MC. SWISS-MODEL and the Swiss-PdbViewer: an environment for comparative protein modeling. Electrophoresis 1997;18:2714–2723.
21. Martz E. Protein explorer: easy yet powerful macromolecular visualization. Trends Biochem Sci 2002;27:107–109.
22. Arrondo JLR, Muga A, Castresana J, Goni FM. Quantitative studies of the structure of proteins in solutions by Fourier-transform infrared spectroscopy. Prog Biophys Mol Biol 1993;59:23–56.
23. Krimm S, Bandekar J. Vibrational spectroscopy and conformation of peptides, polypeptides, and proteins. Adv Protein Chem 1986;38:181–364.
24. Barth A. The infrared absorption of amino acid side chains. Prog Biophys Mol Biol 2000;74:141–173.
25. Osborne HB, Nabedryk-Viala E. Infrared measurements of peptide hydrogen exchange in rhodopsin. Methods Enzymol 1982;88: 676–680.
26. D'Auria S, Barone R, Rossi M, Nucci R, Barone G, Fessas D, Bertoli E, Tanfani F. Effects of temperature and SDS on the structure of β-glycosidase from the thermophilic archaeon *Sulfolobus Solfataricus*. Biochem J 1997;323:833–840.
27. Herman P, Staiano M, Marabotti A, Varriale A, Scirè A, Tanfani F, Vecer J, Rossi M, D'Auria S. D-Trehalose/D-maltose-binding protein from the hyperthermophilic archaeon *Thermococcus litoralis*. The binding of trehalose and maltose results in different protein conformational states. Proteins 2006;63:754–767.
28. Bauer MW, Kelly RM. The family 1 beta-glucosidases from Pyrococcus furiosus and Agrobacterium faecalis share a common catalytic mechanism. Biochemistry 1998;37:17170–17178.
29. Skorko-Glonek J, Lipinska B, Krzewski K, Zolese G, Bertoli E, Tanfani F. HtrA heat-shock protease interacts with phospholipid membranes and undergoes conformational changes. J Biol Chem 1997;272:8974–8982.
30. Scirè A, Saccucci F, Bertoli E, Cambria MT, Principato G, D'Auria S, Tanfani F. Effect of acidic phospholipids on the structural properties of recombinant cytosolic human glyoxalase II. Proteins 2002;48:126–133.
31. Muga A, Arrondo JL, Bellon T, Sancho J, Bernabeu C. Structural and functional studies on the interaction of sodium dodecyl sulfate with beta-galactosidase. Arch Biochem Biophys 1993;300:451–457.
32. Gloster TM, Roberts S, Ducros VM, Perugino G, Rossi M, Hoos R, Moracci M, Vasella A, Davies GJ. Structural studies of the β-glycosidase from *Sulfolobus solfataricus* in complex with covalently and noncovalently bound inhibitors. Biochemistry 2004;43: 6101–6109.
33. Kaper T, Lebbink JH, Pouwels J, Kopp J, Schulz GE, van der Oost J, de Vos WM. Comparative structural analysis and substrate specificity engineering of the hyperthermostable beta-glucosidase CelB from *Pyrococcus furiosus*. Biochemistry 2000;39: 4963–4970.
34. Karshikoff A, Ladenstein R. Ion pairs and the thermotolerance of proteins from hyperthermophiles: a "traffic rule" for hot roads. Trends Biochem Sci 2001;26:550–556.
35. Bueno M, Cremades N, Neira JL, Sancho J. Filling small, empty protein cavities: structural and energetic consequences. J Mol Biol 2006;358:701–712.
36. Jackson SE, Moracci M, elMasry N, Johnson CM, Fersht AR. Effect of cavity-creating mutations in the hydrophobic core of chymotrypsin inhibitor 2. Biochemistry 1993;32:11259–11269.
37. Buckle AM, Cramer P, Fersht AR. Structural and energetic responses to cavity-creating mutations in hydrophobic cores: observation of a buried water molecule and the hydrophilic nature of such hydrophobic cavities. Biochemistry 1996;35:4298–42305.
38. Pedone E, Saviano M, Bartolucci S, Rossi M, Ausili A, Scirè A, Bertoli E, Tanfani F. Temperature-, SDS-, and pH-induced conformational changes in protein disulfide oxidoreductase from the archaeon Pyrococcus furiosus: a dynamic simulation and fourier transform infrared spectroscopic study. J Proteome Res 2005;4: 1972–1980.
39. Sayle RA, Milner-White EJ. RASMOL: biomolecular graphics for all. Trends Biochem Sci 1995;20:374–376.